Supporting Information

Sodium Ion Storage Properties of WS$_2$-Decorated Three-Dimensional Reduced Graphene Oxide Microspheres

Seung Ho Choi and Yun Chan Kang[*]

Department of Materials Science and Engineering, Korea University, Anam-Dong, Seongbuk-Gu, Seoul 136-713, Republic of Korea.

*Corresponding author. Fax: (+82) 2-928-3584.

E-mail address: yckang@korea.ac.kr

Experimental Section

Synthesis method. Graphene oxide (GO) was synthesized using a modified Hummer's method. The as-obtained GO was redispersed in distilled water and exfoliated by ultrasonication to generate GO sheets, and 500 mL of the exfoliated GO solution (1 mg ml^{-1}) was added to 1.5 g of ammonium tungstate hydrate. Then, 3.0 g of 100 nm-sized PS nanobeads was added to the solution of GO sheets and W salt. The resulting solution was dispersed in distilled water by ultrasonication. WO_3-3D RGO microspheres were directly prepared by ultrasonic spray pyrolysis at 800°C. A quartz reactor of length 1200 mm and diameter 50 mm was used, with a nitrogen flow rate (carrier gas) of 5 L min^{-1}. The WO_3-3D RGO microspheres were sulfidated at 400 °C for 12 h in the presence of 10% H_2/Ar mixture gas with thiourea as a sulfur source. An alumina boat containing the WO_3-3D RGO microspheres powders was loaded into a larger alumina boat with a cover. A thiourea powder was loaded on the outside of the small alumina boat for complete sulfidation of the WO_3-3D RGO microspheres. Decomposition of the melted thiourea under hydrogen/argon mixture gas supplied as the carrier gas produced hydrogen sulfide gas. Finally, the WS_2-3D RGO microspheres were produced by sulfidation of the WO_3-3D RGO microspheres thanks to the hydrogen sulfide gas continuously generated by thiourea. The 3D RGO, WO_3, WS_2, and WS_2-RGO microspheres were also prepapred for comparison. The bare WO_3 and WO_3-RGO powders were directly prepared by spray pyrolysis from the spray solutions with and without GO sheets, respectively. The bare WS_2 and WS_2-RGO powders were obtained by sulfidation process of bare WO_3 and WO_3-RGO powders, respectively. The 3D RGO microspheres were directly prepared by spray pyrolysis from the spray solution with GO sheets and PS nanobeads.

Characterizations. The crystal structures of the microspheres were investigated by X-ray diffractometry (XRD, X'pert PRO MPD), using Cu Kα radiation ($\lambda = 1.5418$ Å). Morphological features were investigated using field-emission scanning electron microscopy (FE-SEM, Hitachi S-4800) and high-resolution transmission electron microscopy (HR-TEM, JEM-2100F) at a working voltage of 200 kV. The specific surface areas of the microspheres were calculated from a Brunauer–Emmett–Teller (BET) analysis of nitrogen adsorption measurements (TriStar 3000). The microspheres were also investigated using X-ray photoelectron spectroscopy (XPS, ESCALAB-210) with Al Kα radiation (1486.6 eV). Thermal gravimetric analysis (TGA, SDT Q600) was performed in air at a heating rate of 10°C min^{-1} to determine the amount of carbon in the microspheres.

Electrochemical measurements. The capacities and cycling properties of the WS_2-3D RGO and WO_3-3D RGO microspheres were determined using 2032-type coin cells. The electrodes were prepared from a mixture containing 70 wt% active material, 20 wt% Super P, and 10 wt% sodium carboxymethyl cellulose (Na-CMC) binder. Sodium metal and microporous polypropylene film were used as a counter electrode and separator, respectively. The electrolyte was a solution of 1 M $NaClO_4$ (Aldrich) in a 1:1 volume mixture of ethylene carbonate/dimethyl carbonate (EC/DMC) to which 5 wt% fluoroethylene carbonate was added. The charge-discharge characteristics of the samples were determined by cycling in the potential range 0.001–3.0 V at fixed current densities. Cyclic voltammetry (CV) was carried out at a scan rate of 0.1 mV s^{-1}. The dimensions of the negative electrode were 1 cm × 1 cm and the mass loading was approximately 1.4 mg cm^{-2}. Electrochemical impedance was measured using electrochemical impedance spectroscopy (EIS) over a frequency range of 0.01 Hz–100 kHz.
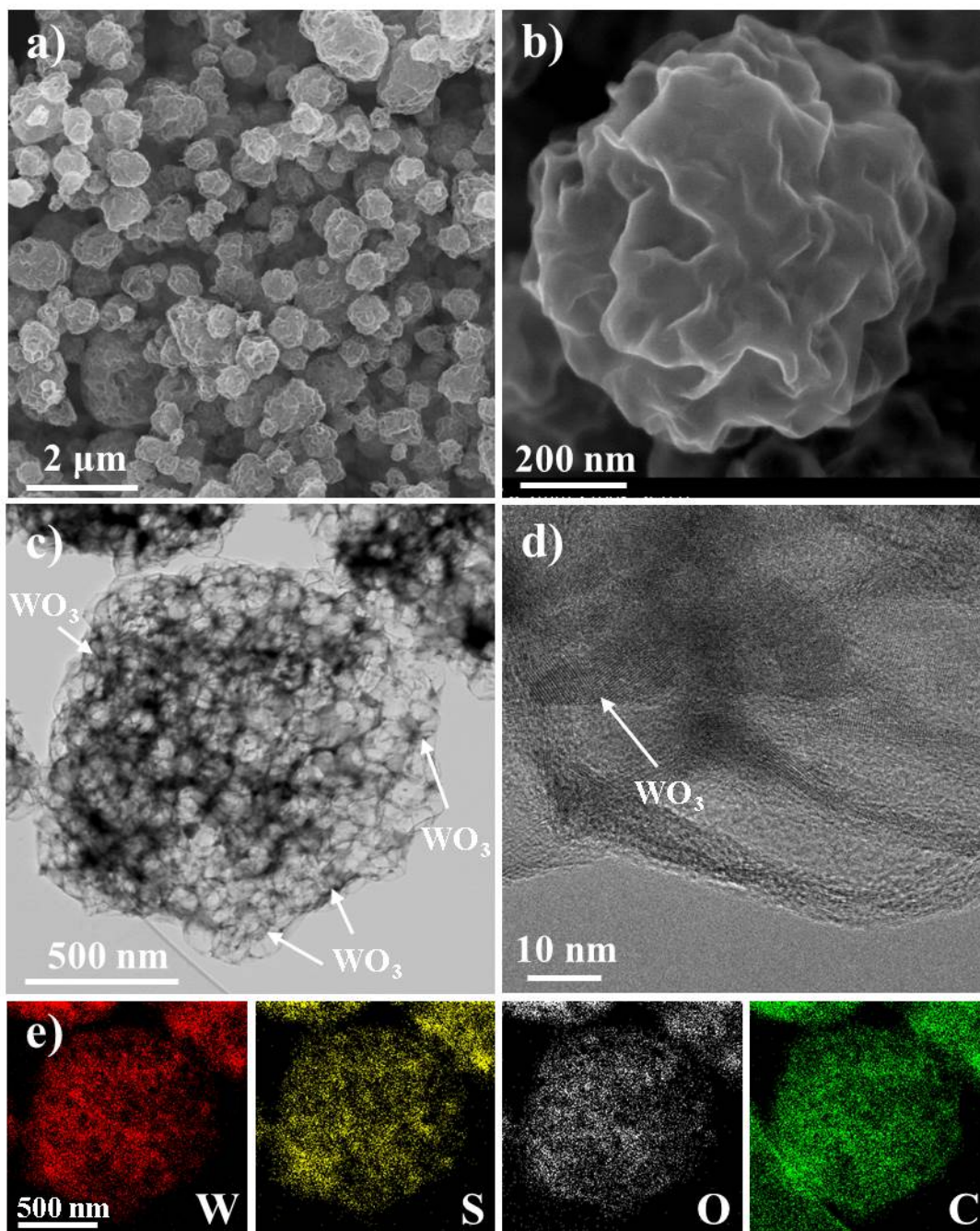
Fig. S1 Morphologies of the WO_3-3D RGO microspheres obtained at a sulfidation temperature of 200°C. a,b) FE-SEM images, c,d) TEM images, and e) elemental mapping images of W, S, O, and C components.
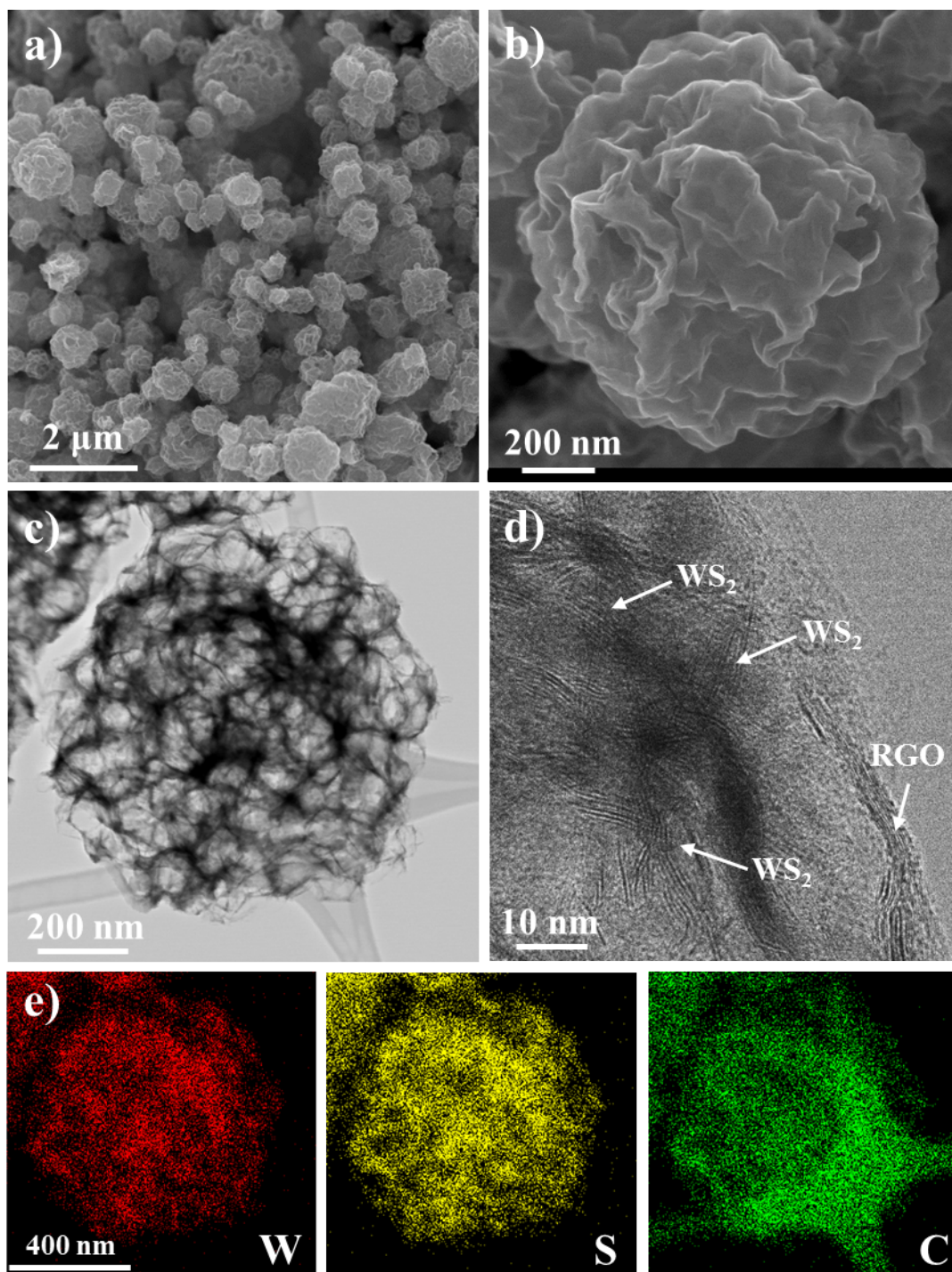
4

Fig. S2 Morphologies of the WS$_2$-3D RGO microspheres obtained at a sulfidation temperature of 600°C. a,b) FE-SEM images, c,d) TEM images, and e) elemental mapping images of W, S, and C components.
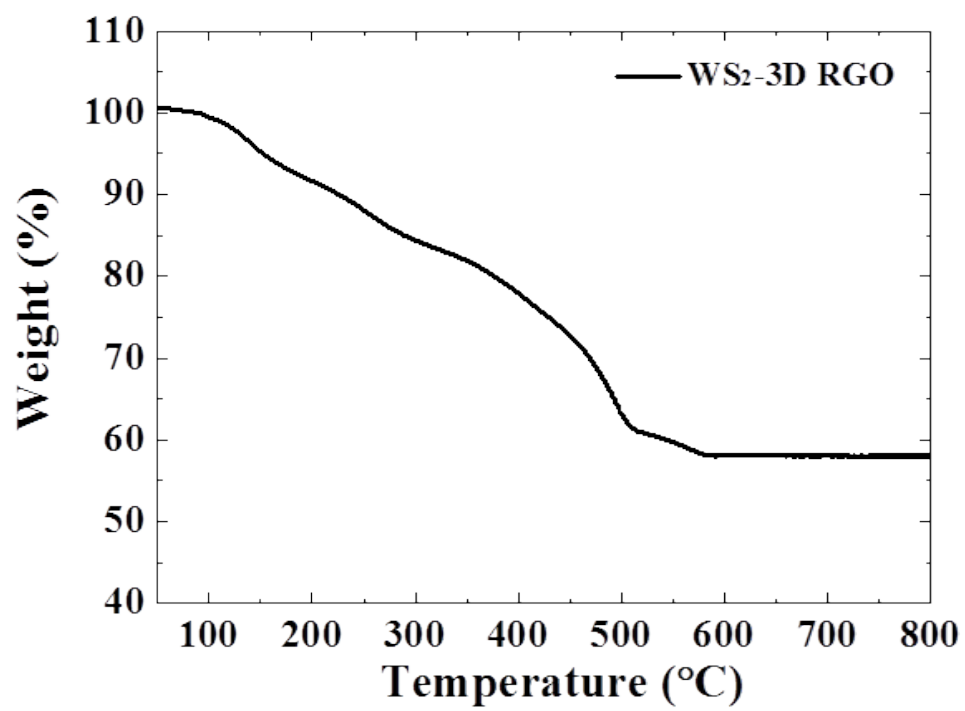
5

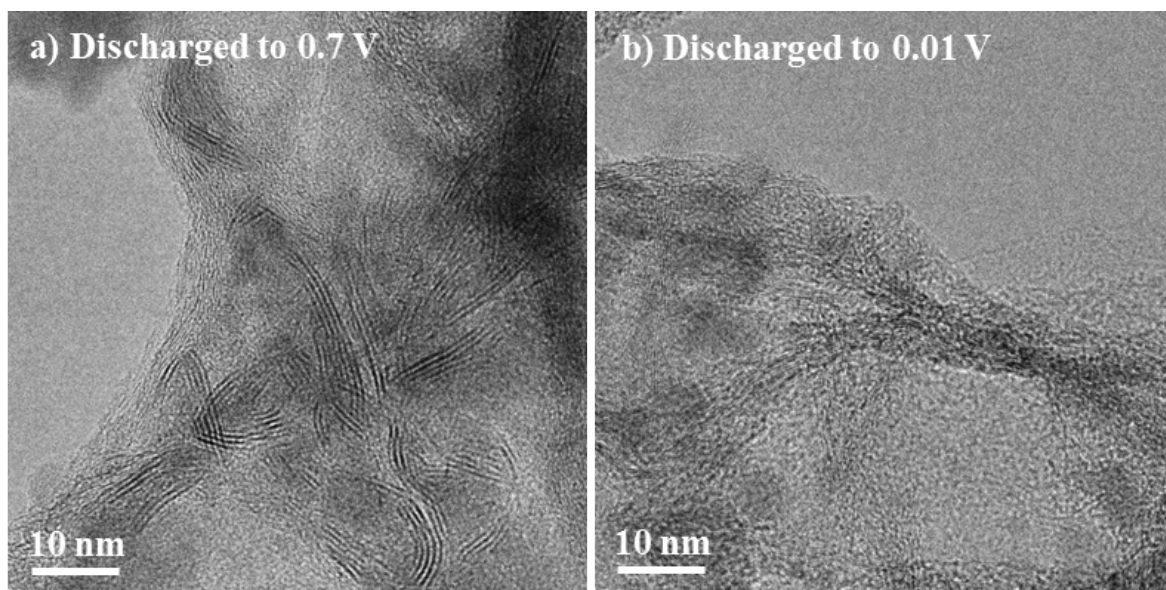**Fig. S3** TG curve of the WS$_2$-3D RGO microspheres.

Fig. S4 High resolution TEM images of the WS$_2$-3D RGO microspheres obtained after first discharge process to (a) 0.7 V and (b) 0.01 V.
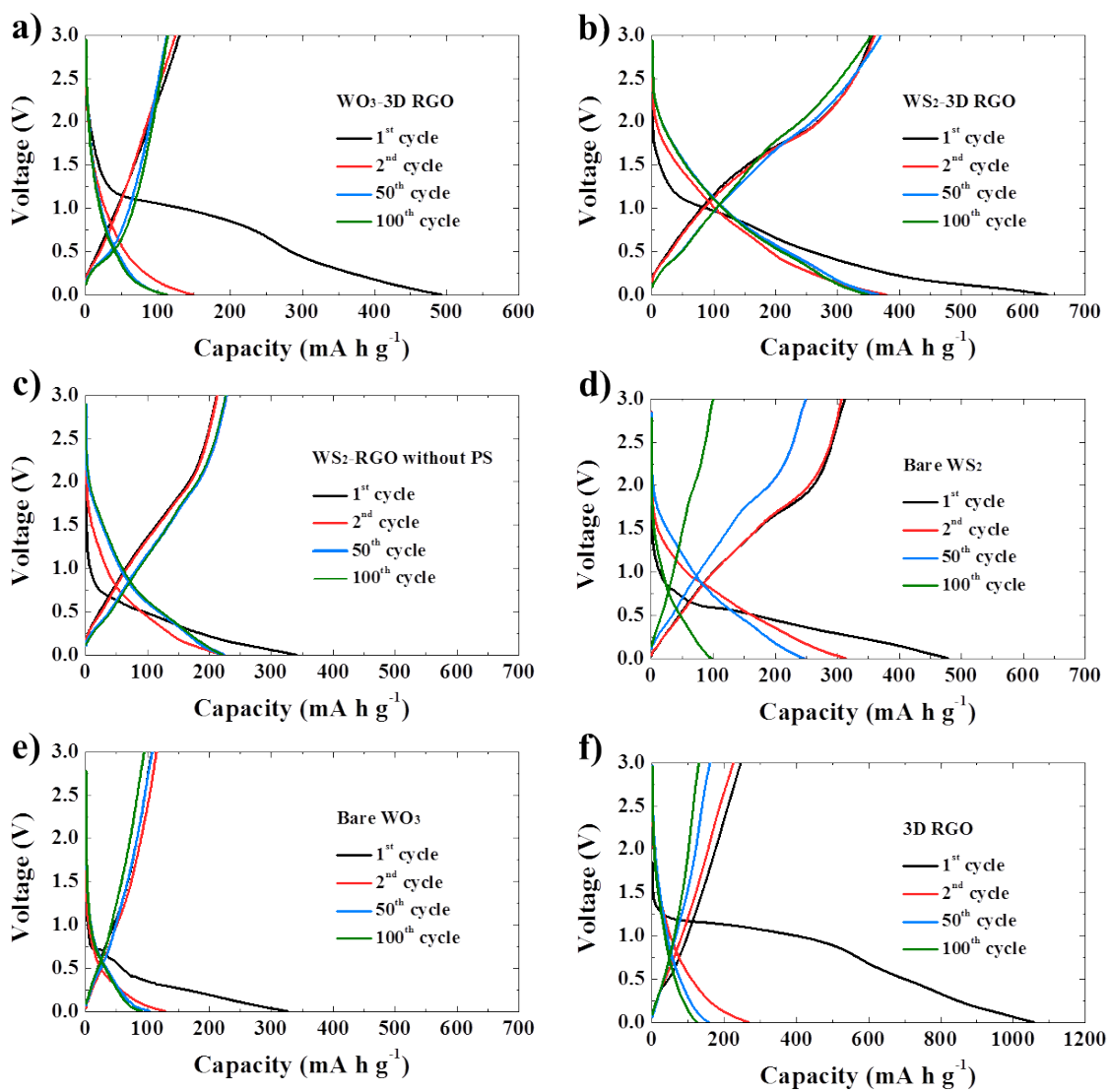
Fig. S5 Charge and discharge curves of the microspheres at a current density of 200 mA g^{-1}. a) WO$_3$-3D RGO, b) WS$_2$-3D RGO, c) WS$_2$-RGO, d) Bare WS$_2$, e) bare WO$_3$, and f) 3D RGO.
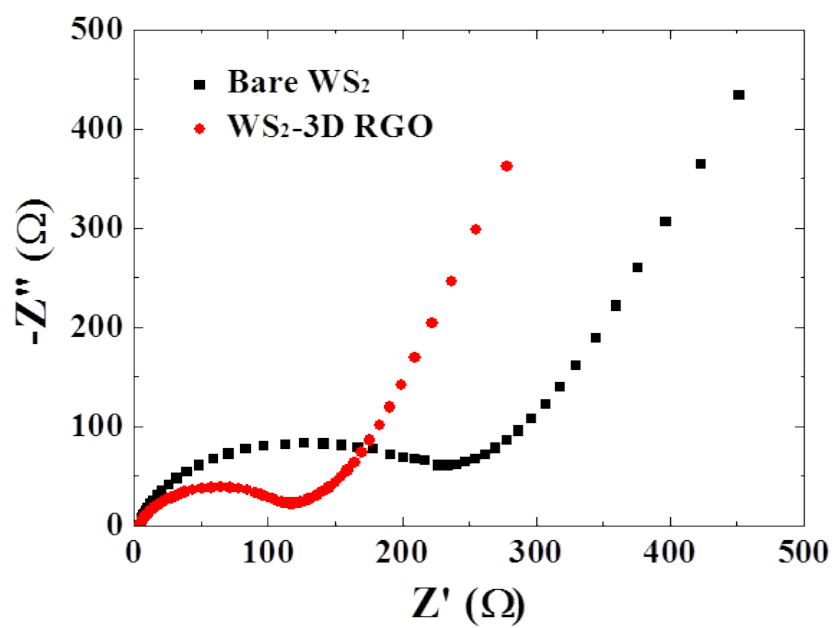
Fig. S6 Electrochemical impedance spectroscopy (EIS) of the WS$_2$-3D RGO and bare WS$_2$ microspheres.
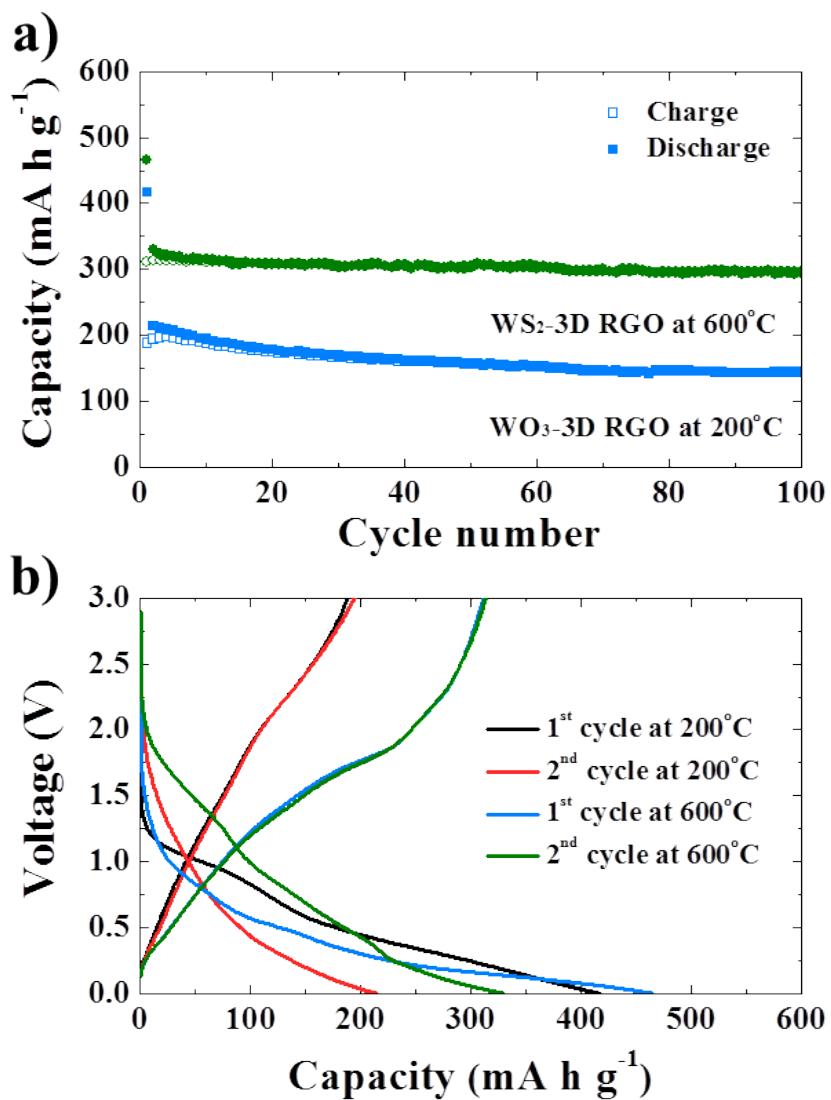
Fig. S7 Cycling performances and charge/discharge curves of the microspheres obtained at sulfidation temperatures of 200 °C and 600 °C. a) cycling performances and b) first and second cycle curves.
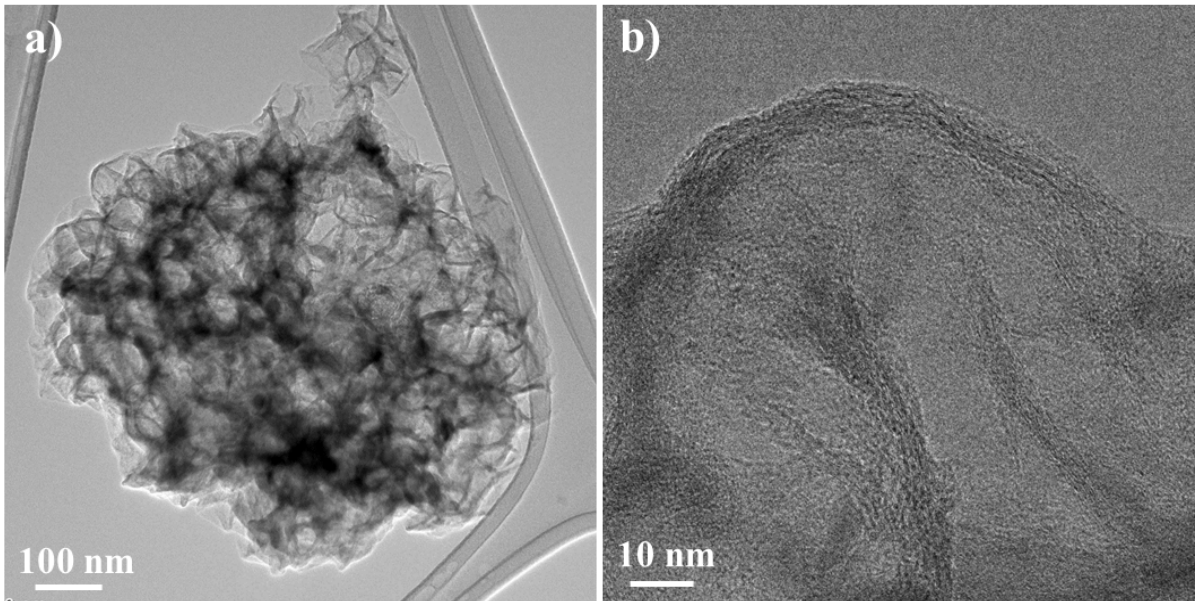
Fig. S8 TEM images of the WS$_2$-3D RGO microsphere obtained after rate performance test.

Table S1 – Na$^+$ storage properties of various WS$_2$ and MoS$_2$ materials on copper foil.			
Typical examples	Synthesis	Electrochemical properties	Ref
WS$_2$@graphene nanocomposites	Hydrothermal approach	340 mA h g^{-1} after 500 cycles at 20 mA g^{-1} 150 mA h g^{-1} after 200 cycles at 320 mA g^{-1}	[1]
MoS$_2$/Graphene Composite Paper	Vacuum filtration	218 mA h g^{-1} after 20 cycles at 25 mA g^{-1}	[2]
MoS$_2$ Embedded in Carbon Nanofibers	Electrospinning process	300 mA h g^{-1} after 100 cycles at 1000 mA g^{-1}	[3]
MoS$_2$/Graphene Composites	Hydrothermal method	312.7 mA h g^{-1} after 200 cycles at 100 mA g^{-1}	[4]
Vine-like MoS$_2$ Fiber	Electrospinning process	470 mA h g^{-1} after 30 cycles at 100 mA g^{-1}	[5]
MoS$_2$/Carbon Composite	Hydrothermal method	400 mA h g^{-1} after 300 cycles at 670 mA g^{-1}	[6]
MoS$_2$ Nanoflowers	Hydrothermal method	320 mA h g^{-1} after 600 cycles at 200 mA g^{-1}	[7]
Ultrathin MoS$_2$ Nanosheets	Ultrasonic exfoliation technique	251 mA h g^{-1} after 100 cycles at 320 mA g^{-1}	[8]
WS$_2$@3D RGO Compsoite	Spray pyrolysis	334 mA h g^{-1} after 200 cycles at 200 mA g^{-1} and 287 mA h g^{-1} at 900 mA g^{-1}	This work

[1] D. Su, S. Dou and G. Wang, Chem. Commun., 2014, 50, 4192–4195.

[2] L. David, R. Bhandavat and G. Singh, ACS Nano, 2014, 8, 1759–1770.

[3] C. Zhu, X. Mu, P. A. van Aken, Y. Yu and J. Maier, Angew. Chem. Int. Ed., 2014, 53, 2152–2156.

[4] Y. X. Wang, S. L. Chou, D. Wexler, H. K. Liu and S. X. Dou, Chem. Eur. J., 2014, 20, 9607–9612.

[5] W. H. Ryu, J. W. Jung, K. Park, S. J. Kim and I. D. Kim, Nanoscale, 2014, 6, 10975–10981.

[6] J. Wang, C. Luo, T. Gao, A. Langrock, A. C. Mignerey and C. Wang, Small, 2014, DOI: 10.1002/smll.201401521.

[7] Z. Hu, L. Wang, K. Zhang, J. Wang, F. Cheng, Z. Tao and J. Chen, Angew. Chem. Int. Ed., 2014, 53, 12794–12798.

[8] D. Su, S. Dou and G. Wang, Adv. Energy Mater. 2014, 1401205.